The Astronomical Journal, 130:234–245, 2005 July

OPTICAL PHOTOMETRY AND SPECTROSCOPY OF THE SUSPECTED "COOL ALGOL" AV DELPHINI: DETERMINATION OF THE PHYSICAL PROPERTIES

Jeff A. Mader,[1] Guillermo Torres,[2] Laurence A. Marschall,[3] and Akbar Rizvi[3]

Received 2005 January 25; accepted 2005 March 16

ABSTRACT

We present new spectroscopic and *BVRI* photometric observations of the double-lined eclipsing binary AV Del (period = 3.85 days) conducted over six observing seasons. A detailed radial velocity and light-curve analysis of the optical data shows the system to be most likely semidetached, with the less massive and cooler star filling its Roche lobe. The system is probably a member of the rare class of "cool Algol" systems, which are distinguished from the "classical" Algol systems in that the mass-gaining component is also a late-type star rather than a B- or A-type star. By combining the spectroscopic and photometric analyses, we derive accurate absolute masses for the components of $M_1 = 1.453 \pm 0.028\ M_\odot$ and $M_2 = 0.705 \pm 0.014\ M_\odot$ and radii of $R_1 = 2.632 \pm 0.030\ R_\odot$ and $R_2 = 4.233 \pm 0.060\ R_\odot$, as well as effective temperatures of 6000 ± 200 and 4275 ± 150 K for the primary and secondary, respectively. There are no obvious signs of activity (spottedness) in the optical light curve of the binary.

Key words: binaries: eclipsing — binaries: spectroscopic — stars: fundamental parameters — stars: individual (AV Delphini)

Online material: machine-readable tables

1. INTRODUCTION

The class of interacting binaries known as the classical Algols are semidetached systems that contain a late-type giant or subgiant star that fills its Roche lobe and is transferring mass onto a much more luminous and more massive B–A main-sequence star. This paper continues our study of the new class of binaries referred to as "cool Algols." These systems were first recognized by Popper (1992) and are binaries with properties that are similar to those of classical Algols, except that the mass-gaining component is a late-type giant or subgiant like its companion. They typically display signs of magnetic activity in the form of Ca II H and K emission, Hα emission, starspots, and strong X-ray emission. Only about a dozen cool Algols are known, and many of them were mistakenly assigned to the larger group of RS Canum Venaticorum (RS CVn) binaries that contain a luminous K-type primary with a fainter F–G-type companion. The main difference between the cool Algols and the RS CVn systems is that the latter are detached (see, e.g., Popper 1980; Hall 1989).

The general characteristics of the cool Algols are fairly well defined (see Popper 1992; Torres et al. 1998) but accurate information on individual systems is still far from complete. Only six of the members have spectroscopic orbits for both components (RZ Cnc, AR Mon, RT Lac, AD Cap, RV Lib, and BD +05°706; Popper 1976, 1991; Torres et al. 1998; Williamon et al. 2005). All of these systems, with the exception of RV Lib, have had light-curve analyses performed on them that have yielded the absolute masses and radii necessary in order to understand their properties. The remaining objects listed as possible members of this class (UZ Cnc, V1061 Cyg, AV Del, GU Her, and V756 Sco; Popper 1996) have very little in the way of observations, and in some cases even the orbital periods are poorly known. Detailed studies of most of these are currently underway and will be the subject of future papers.

AV Delphini ($\alpha = 20^{\rm h}45^{\rm m}31\overset{\rm s}{.}47$, $\delta = +11^\circ10'26\overset{''}{.}4$, J2000.0; $V = 11.8$) is a rather neglected variable star discovered by Hoffmeister (1935) and given the original designation 184.1930. It is a suspected member of the cool Algols (Popper 1996) and was reported by that author as a double-lined system with a period of 3.85 days and a mean spectral type of G5, although other sources have classified it as F8 (e.g., Halbedel 1984). We present here a full *BVRI* photometric and spectroscopic analysis of this system yielding accurate absolute masses and radii, along with other physical properties.

2. EPHEMERIS

Times of eclipse have been recorded for AV Del over more than seven decades since its discovery. Unfortunately, only two recent measurements are photoelectric, while the remaining ones are either visual or photographic[4] and thus have much larger uncertainties. All are of the primary minimum, since the secondary eclipse is very shallow. The time sampling of our own photometric observations is inadequate for determining additional eclipse timings from single events, but when taken together the data allow us to establish an average time of primary minimum, as we describe below in § 5. Similarly, our radial velocity measurements yield another average estimate that is also useful. We collect these and all other timings in Table 1, where the uncertainties are given as published or were assigned from the scatter of each type of measurement. A fit to the 28 minima gives the linear ephemeris

$$\text{Min. I (HJD)} = 2{,}450{,}714.34779(39) + 3.8534528(35)E, \quad (1)$$

[1] W. M. Keck Observatory, 65-1120 Mamalahoa Highway, Kamuela, HI 96743; jmader@keck.hawaii.edu.

[2] Harvard-Smithsonian Center for Astrophysics, 60 Garden Street, Cambridge, MA 02138; gtorres@cfa.harvard.edu.

[3] Department of Physics, Gettysburg College, 300 North Washington Street, Gettysburg, PA 17325; marschal@gettysburg.edu.

[4] The photographic measurements are actually only times of "low light," since the plates are typically too sparse to cover the minimum with any degree of completeness. Nevertheless, they do constrain the period (albeit with a precision for a single measurement of only ~0.1 day), since they precede all other timings by nearly three decades.

TABLE 1
TIMES OF PRIMARY MINIMUM FOR AV DEL

HJD (2,400,000+)	Year	Type[a]	E	$(O-C)$ (days)	Reference
25921.292 ± 0.13	1929.8461	pg	−6434	+0.0595	1
26206.385 ± 0.13	1930.6267	pg	−6360	−0.0030	1
26545.486 ± 0.13	1931.5551	pg	−6272	−0.0059	1
27393.5 ± 0.13	1933.8768	pg	−6052	+0.2485	1
27624.469 ± 0.13	1934.5092	pg	−5992	+0.0104	1
27655.425 ± 0.13	1934.5939	pg	−5984	+0.1387	1
27713.3 ± 0.13	1934.7524	pg	−5969	+0.2119	1
38294.71 ± 0.023	1963.7227	v	−3223	+0.0406	2
41901.524 ± 0.023	1973.5976	v	−2287	+0.0228	3
42899.543 ± 0.023	1976.3300	v	−2028	−0.0025	4
42953.515 ± 0.023	1976.4778	v	−2014	+0.0211	5
43458.311 ± 0.023	1977.8599	v	−1883	+0.0148	6
43662.551 ± 0.023	1978.4190	v	−1830	+0.0218	7
43689.515 ± 0.023	1978.4929	v	−1823	+0.0117	7
46321.397 ± 0.023	1985.6986	v	−1140	−0.0146	8
46348.384 ± 0.023	1985.7724	v	−1133	−0.0018	9
46348.386 ± 0.023	1985.7724	v	−1133	+0.0002	9
47003.441 ± 0.023	1987.5659	v	−963	−0.0318	10
47003.465 ± 0.023	1987.5660	v	−963	−0.0078	10
47030.426 ± 0.023	1987.6398	v	−956	−0.0209	10
47057.43 ± 0.023	1987.7137	v	−949	+0.0089	11
48448.502 ± 0.006	1991.5223	v	−588	−0.0155	12
49211.450 ± 0.023	1993.6111	v	−390	−0.0512	10
49211.475 ± 0.008	1993.6112	v	−390	−0.0262	13
50714.3478 ± 0.0003	1997.7258	pe	0	+0.0000	14
51400.278 ± 0.011	1999.6038	pe	+178	+0.0155	15
51889.6472 ± 0.0045	2000.9438	sp	+305	−0.0037	15
52105.4476 ± 0.0021	2001.5344	pe	+361	+0.0033	16

[a] pg = photographic, v = visual, pe = photoelectric, sp = spectroscopic.

REFERENCES.—(1) Hoffmeister et al. 1938; (2) Kordylewski 1963; (3) Diethelm 1973; (4) Diethelm 1976a; (5) Diethelm 1976b; (6) Diethelm 1977; (7) Diethelm 1978; (8) Diethelm 1985; (9) Diethelm 1986; (10) Kundera 2004; (11) Diethelm 1988; (12) Diethelm 1991; (13) Diethelm 1994; (14) Agerer & Hübscher 1999; (15) this paper; (16) Zejda 2004.

where E is the number of cycles counted from the epoch of reference and the uncertainties are given in parentheses in units of the last significant digit. The $O - C$ diagram of all observations is shown in Figure 1. A period study of AV Del was carried out recently by Qian (2002) on the basis of fewer times of eclipse. In particular, the most recent photoelectric timing, as well as one visual and all older photographic observations, was not included. A small period increase of about $3.15 \pm 0.19 \times 10^{-6}$ days yr^{-1} was reported by Qian (2002), which depends strongly on the single photoelectric measurement from 1997 (first of the circles in the figure), giving a more positive residual than the older measurements in his analysis. A new quadratic fit to all the minima in Table 1 gives

$$\text{Min. I (HJD)} = 2{,}450{,}714.34771(34) + 3.8534620(42)\,E + 0.50(16) \times 10^{-8} E^2, \quad (2)$$

in which the second-order term is now smaller and less significant than in Qian's study and corresponds to a period change of $+(0.95 \pm 0.30) \times 10^{-6}$ days yr^{-1}. This period increase, if real, may be related to the mass transfer presumably taking place in the system. Further precise measurements of the times of eclipse are needed to confirm the effect. For the remainder of this paper, we adopt the linear ephemeris in equation (1).

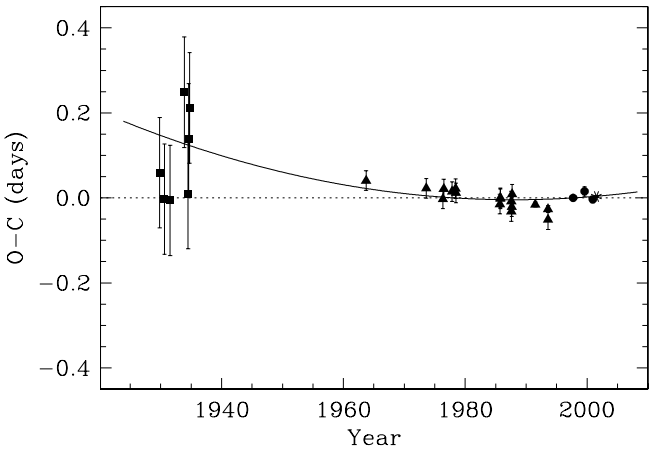

FIG. 1.—$O - C$ diagram based on the linear ephemeris from eq. (1) and all available times of primary eclipse for AV Del. Photographic, visual, photoelectric, and spectroscopic measurements are represented with squares, triangles, circles, and an asterisk, respectively. The curved line represents the parabolic fit in eq. (2), which describes a tentative period increase with time (see text).

3. OBSERVATIONAL MATERIAL

AV Del was observed spectroscopically at the Harvard-Smithsonian Center for Astrophysics (CfA) from 1998 July through 2003 November, using an echelle spectrograph on the 1.5 m Tillinghast reflector at the F. L. Whipple Observatory on Mount Hopkins (Arizona). A single echelle order centered

TABLE 2
PROGRAM STARS

Star	Identification	R.A. (J2000.0)	Decl. (J2000.0)	Spectral Type	V	$B-V$
AV Del	GSC 01093-01255	20 45 31.47	+11 10 26.4	F8	11.8	0.55
Comparison	GSC 01093-01575	20 45 25.58	+11 24 05.3	...	10.90 ± 0.08	1.12 ± 0.17
Check	GSC 01093-01259	20 45 39.45	+11 13 41.0	...	12.8	...

NOTE.—Units of right ascension are hours, minutes, and seconds, and units of declination are degrees, arcminutes, and arcseconds.

around 5187 Å was recorded using a photon-counting Reticon detector, giving 45 Å of coverage at a resolving power of $\lambda/\Delta\lambda \sim 35{,}000$. One further observation was collected with a nearly identical instrument on the 1.5 m Wyeth reflector at the Oak Ridge Observatory at Harvard University (Massachusetts). A total of 68 usable spectra were obtained, with signal-to-noise ratios ranging from about 10 to 30 per resolution element of 8.5 km s^{-1}. The reductions to obtain radial velocities are described in § 4.

Photometric imaging of AV Del was conducted between 1998 August and 1999 January at Gettysburg College Observatory, Gettysburg (Pennsylvania), using a 16 inch (40 cm) f/11 Ealing Cassegrain reflector. The detector was a Photometrics thermoelectrically cooled CCD camera with a front-illuminated Thompson 7896 1024 × 1024 chip and standard Bessell *BVRI* filters. Observations were also made in 1998 October at the 0.8 m telescope of Lowell Observatory on Anderson Mesa, Flagstaff (Arizona), operated by the National Undergraduate Research Observatory (NURO). The NURO detector was a Photometrics LN2-cooled camera with a TEK 512 × 512 back-illuminated chip and, as at Gettysburg, standard Bessell *BVRI* filters. Image reduction for both sets of data was performed using IRAF,[5] and photometric measurements were made using MIRA[6] software. Although the field of view of the two telescopes differed (15′ at Gettysburg and 4′ at NURO), comparison and check stars comparable in color and brightness were available in close proximity to AV Del and thus were easily visible in all the images. In addition,

[5] IRAF is distributed by NOAO, which is operated by the Association of Universities for Research in Astronomy, Inc., under contract to the NSF.
[6] MIRA is a registered trademark of Axiom Research, Inc.

TABLE 3
DIFFERENTIAL MAGNITUDES IN THE *B* BAND (VARIABLE MINUS COMPARISON)

HJD (2,450,000+)	ΔB (mag)	HJD (2,450,000+)	ΔB (mag)	HJD (2,450,000+)	ΔB (mag)	HJD (2,450,000+)	ΔB (mag)
1046.6452	0.339	1096.6837	0.348	1108.5359	0.336	2099.8018	0.449
1054.6922	0.363	1096.7009	0.336	1109.5143	0.437	2099.8495	0.428
1057.6112	0.416	1096.7154	0.339	1110.4943	0.355	2099.8762	0.428
1059.5852	0.401	1096.7449	0.341	1111.5128	0.480	2100.7484	0.342
1061.5762	0.411	1096.7581	0.341	1111.6524	0.356	2100.8133	0.350
1061.7827	0.362	1097.5881	0.446	1112.4967	0.373	2101.7459	0.987
1067.6544	0.352	1097.6002	0.432	1114.5168	0.402	2101.7504	0.943
1068.5904	0.487	1097.6052	0.449	1116.4838	0.370	2101.8464	0.485
1068.7376	1.175	1097.6188	0.451	1117.4948	0.371	2101.8509	0.460
1070.5625	0.446	1097.6330	0.454	1118.4798	0.405	2102.7076	0.343
1075.5378	0.350	1097.6466	0.467	1127.5446	0.325	2102.7121	0.343
1079.5632	0.366	1097.6734	0.476	1129.4807	0.311	2102.7459	0.325
1080.5550	1.115	1097.6834	0.480	1130.4748	1.679	2103.7042	0.445
1083.6049	0.357	1097.6938	0.490	1133.5005	0.344	2103.7086	0.442
1083.7306	0.365	1097.7041	0.489	1136.4923	0.415	2103.7448	0.469
1085.5458	0.354	1097.7172	0.491	1140.5204	0.438	2103.8159	0.395
1086.5504	0.406	1097.7269	0.494	1142.4701	0.385	2103.8204	0.400
1088.6498	0.373	1097.7378	0.501	1149.5195	0.470	2118.8864	0.484
1089.5316	0.384	1097.7489	0.494	1157.4543	1.795	2119.6883	0.337
1095.6550	0.798	1097.7639	0.506	1162.4576	0.336	2119.7169	0.352
1095.6775	0.912	1098.6167	0.332	1164.4517	0.360	2119.8334	0.326
1095.6911	1.008	1098.7070	0.329	1166.4417	0.371	2119.8675	0.319
1095.7027	1.118	1098.7209	0.335	1170.4506	0.400	2120.6888	0.832
1095.7104	1.162	1098.7354	0.340	1173.4516	0.374	2120.7250	1.052
1095.7167	1.231	1099.6210	1.641	1178.4463	0.414	2120.7789	1.508
1095.7264	1.334	1099.6353	1.746	1179.4580	0.328	2120.8127	1.746
1095.7334	1.376	1100.5919	0.335	2097.7987	1.689	2120.8525	1.917
1095.7569	1.573	1100.6099	0.345	2097.8358	1.405	2120.8715	1.891
1095.7669	1.651	1101.5920	0.493	2097.8611	1.184	2121.6971	0.352
1095.7782	1.747	1101.6221	0.502	2098.7235	0.320	2121.7577	0.345
1095.7866	1.788	1102.5233	0.349	2099.7046	0.492	2121.7943	0.337
1095.7925	1.824	1103.6010	1.716	2099.7499	0.483	2121.8517	0.336
1096.6038	0.349	1107.5044	1.257	2099.7715	0.471	2122.7142	0.470

Table 3 is also available in machine-readable form in the electronic edition of the *Astronomical Journal*.

TABLE 4

DIFFERENTIAL MAGNITUDES IN THE V BAND (VARIABLE MINUS COMPARISON)

HJD (2,450,000+)	ΔV (mag)	HJD (2,450,000+)	ΔV (mag)	HJD (2,450,000+)	ΔV (mag)	HJD (2,450,000+)	ΔV (mag)
1046.6422	0.564	1096.6828	0.583	1107.5006	1.348	2099.8027	0.705
1054.6866	0.591	1096.7000	0.580	1108.5328	0.567	2099.8504	0.719
1055.6571	0.665	1096.7144	0.578	1109.5112	0.685	2099.8771	0.689
1057.6084	0.630	1096.7440	0.574	1110.4915	0.575	2100.7493	0.594
1058.5789	0.572	1096.7572	0.575	1111.5100	0.695	2100.8142	0.582
1059.5819	0.657	1097.5871	0.712	1111.6484	0.634	2101.7469	1.151
1061.5726	0.625	1097.5992	0.714	1112.4937	0.591	2101.7513	1.098
1061.7767	0.601	1097.6043	0.712	1114.5141	0.617	2101.8474	0.730
1062.6049	0.571	1097.6179	0.731	1116.4810	0.604	2101.8518	0.717
1067.6511	0.602	1097.6320	0.727	1117.4917	0.604	2102.7085	0.581
1068.7348	1.272	1097.6457	0.748	1118.4771	0.625	2102.7130	0.574
1070.5591	0.686	1097.6725	0.752	1127.5398	0.556	2102.7469	0.591
1075.5337	0.568	1097.6825	0.761	1129.4770	0.564	2103.7051	0.702
1079.5596	0.572	1097.6929	0.775	1130.4706	1.702	2103.7095	0.704
1080.5512	1.254	1097.7032	0.778	1133.4977	0.581	2103.7457	0.668
1083.6011	0.588	1097.7163	0.787	1136.4896	0.678	2103.8168	0.643
1083.7278	0.675	1097.7259	0.789	1140.5163	0.624	2103.8213	0.638
1085.5431	0.589	1097.7369	0.783	1142.4674	0.621	2118.8873	0.788
1086.5474	0.632	1097.7479	0.787	1149.5165	0.682	2119.6892	0.584
1088.6448	0.607	1097.7630	0.789	1157.4515	1.723	2119.7179	0.571
1089.5288	0.612	1097.7728	0.790	1162.4549	0.579	2119.8344	0.562
1095.6541	0.970	1098.6158	0.565	1164.4486	0.597	2119.8684	0.573
1095.6766	1.082	1098.6492	0.581	1166.4382	0.587	2120.6897	1.031
1095.6902	1.162	1098.7061	0.565	1170.4475	0.612	2120.7259	1.211
1095.7017	1.225	1098.7200	0.574	1173.4485	0.604	2120.7798	1.556
1095.7094	1.269	1098.7344	0.571	1178.4502	0.651	2120.8136	1.707
1095.7158	1.316	1099.6201	1.607	1179.4543	0.574	2120.8534	1.804
1095.7255	1.368	1099.6344	1.680	1180.4572	1.020	2120.8725	1.803
1095.7325	1.426	1100.5910	0.563	2097.7996	1.704	2121.6981	0.591
1095.7560	1.562	1100.6089	0.562	2097.8367	1.487	2121.7587	0.576
1095.7660	1.619	1101.5911	0.781	2097.8621	1.309	2121.7952	0.581
1095.7773	1.666	1101.6147	0.778	2098.7244	0.581	2121.8527	0.582
1095.7856	1.704	1101.6212	0.755	2099.7055	0.783	2122.7152	0.781
1095.7916	1.726	1102.5204	0.552	2099.7508	0.743		
1096.6029	0.586	1103.5979	1.698	2099.7725	0.743		

Table 4 is also available in machine-readable form in the electronic edition of the *Astronomical Journal*.

photometric data were obtained during the 2001–2002 observing season at McDonald Observatory in Fort Davis, Texas, with a 30 inch (0.76 m) f/3.0 Cassegrain reflector and a thermoelectrically cooled Loral Fairchild 2048 × 2048 CCD. Bessel *BVRI* filters were used for these data as well.

A total of 132, 138, 139, and 136 photometric observations were made in the *B*, *V*, *R*, and *I* filters, respectively. The comparison and check stars used were GSC 01093-01575 and GSC 01093-01259, respectively. Basic properties for these stars are listed in Table 2. The precision of an individual differential photometric measurement is estimated to be 0.031, 0.012, 0.011, and 0.011 mag in the *B*, *V*, *R*, and *I* passbands, respectively, derived from the comparison and check stars under the assumption that they do not vary. The observations are listed in Tables 3–6. The depth of eclipse in the *V* band is approximately 1.28 mag for the primary minimum and 0.22 mag for the secondary. There are no obvious signs of activity displayed by the system such as unequal brightness at the quadratures (the O'Connell effect) or other significant distortions in the light curve at other phases, which might indicate spots.

4. SPECTROSCOPIC ANALYSIS

Radial velocities for both components were determined using the two-dimensional cross-correlation technique TODCOR (Zucker & Mazeh 1994). In this method the observed spectra are cross-correlated against a linear combination of two different templates, matched to each star of the binary. The templates were selected from a large library of synthetic spectra based on model atmospheres by R. L. Kurucz.[7] The parameters for the optimum templates were determined by running grids of cross-correlations and seeking the maximum correlation value averaged over all exposures. From a preliminary analysis we adopted surface gravities for the primary and secondary of $\log g = 3.5$ and 3.0, respectively, and we assumed solar composition. The effective temperature we estimated for the primary is $T_{\rm eff} = 6000 \pm 200$ K and its projected rotational velocity is $v \sin i = 35 \pm 1$ km s^{-1}. For the secondary we estimated $v \sin i = 56 \pm 3$ km s^{-1} but were unable to derive its temperature from our spectra because of the much weaker and broader lines. Nevertheless, the secondary temperature is well constrained by the photometry through the light-curve solution (see § 5), from which we adopted the value $T_{\rm eff} = 4250$ K. These temperatures explain the apparent discrepancy in the spectral classifications noted in § 1: as pointed out by Popper (1996), his G5 type is based on the strength of the Na I D lines and is dominated by the stronger

[7] See http://cfaku5.cfa.harvard.edu.

TABLE 5

DIFFERENTIAL MAGNITUDES IN THE *R* BAND (VARIABLE MINUS COMPARISON)

HJD (2,450,000+)	ΔR (mag)	HJD (2,450,000+)	ΔR (mag)	HJD (2,450,000+)	ΔR (mag)	HJD (2,450,000+)	ΔR (mag)
1046.6401.....	0.651	1096.6820.....	0.660	1103.5960.....	1.646	2099.7733.....	0.857
1054.6834.....	0.683	1096.6992.....	0.678	1107.4988.....	1.425	2099.8035.....	0.836
1055.6552.....	0.750	1096.7136.....	0.664	1108.5305.....	0.646	2099.8512.....	0.793
1057.6049.....	0.732	1096.7432.....	0.666	1109.5093.....	0.781	2099.8779.....	0.780
1058.5771.....	0.667	1096.7564.....	0.668	1110.4897.....	0.660	2100.7501.....	0.661
1059.5799.....	0.736	1097.5863.....	0.815	1111.5081.....	0.786	2100.8150.....	0.671
1061.5688.....	0.714	1097.5984.....	0.824	1111.6462.....	0.709	2101.7476.....	1.161
1061.7739.....	0.685	1097.6035.....	0.833	1112.4917.....	0.669	2101.7521.....	1.138
1067.6492.....	0.660	1097.6171.....	0.842	1114.5123.....	0.686	2101.8482.....	0.799
1068.5853.....	0.771	1097.6312.....	0.827	1116.4769.....	0.688	2101.8526.....	0.809
1068.7325.....	1.270	1097.6448.....	0.857	1117.4891.....	0.711	2102.7093.....	0.669
1070.5560.....	0.780	1097.6588.....	0.872	1118.4752.....	0.715	2102.7138.....	0.655
1075.5316.....	0.648	1097.6717.....	0.869	1127.5350.....	0.647	2102.7477.....	0.665
1079.5576.....	0.648	1097.6817.....	0.883	1129.4747.....	0.663	2103.7059.....	0.811
1080.5478.....	1.283	1097.6921.....	0.887	1130.4687.....	1.626	2103.7103.....	0.788
1083.5970.....	0.683	1097.7024.....	0.893	1133.4958.....	0.665	2103.7465.....	0.742
1083.7256.....	0.735	1097.7154.....	0.891	1136.4878.....	0.795	2103.8176.....	0.738
1085.5412.....	0.674	1097.7251.....	0.908	1140.5119.....	0.725	2103.8221.....	0.740
1086.5451.....	0.723	1097.7360.....	0.914	1142.4654.....	0.708	2118.8881.....	0.897
1088.6429.....	0.705	1097.7471.....	0.911	1149.5145.....	0.781	2119.6900.....	0.664
1089.5263.....	0.699	1097.7621.....	0.912	1157.4491.....	1.643	2119.7188.....	0.657
1095.6533.....	1.031	1097.7720.....	0.904	1162.4530.....	0.650	2119.8352.....	0.644
1095.6757.....	1.137	1098.6149.....	0.651	1164.4467.....	0.660	2119.8692.....	0.653
1095.6894.....	1.192	1098.6483.....	0.650	1166.4363.....	0.680	2120.6906.....	1.076
1095.7009.....	1.240	1098.7052.....	0.638	1170.4453.....	0.688	2120.7267.....	1.247
1095.7086.....	1.292	1098.7191.....	0.650	1173.4463.....	0.690	2120.7806.....	1.508
1095.7150.....	1.322	1098.7335.....	0.655	1178.4519.....	0.735	2120.8144.....	1.662
1095.7247.....	1.380	1099.6191.....	1.582	1179.4517.....	0.662	2120.8543.....	1.715
1095.7317.....	1.409	1099.6334.....	1.661	1180.4550.....	1.139	2120.8733.....	1.725
1095.7552.....	1.521	1100.5900.....	0.694	2097.8004.....	1.608	2121.6989.....	0.666
1095.7652.....	1.569	1100.6080.....	0.624	2097.8375.....	1.433	2121.7595.....	0.660
1095.7765.....	1.614	1101.5902.....	0.906	2097.8629.....	1.308	2121.7960.....	0.647
1095.7848.....	1.653	1101.6138.....	0.909	2098.7252.....	0.658	2121.8535.....	0.652
1095.7908.....	1.656	1101.6203.....	0.946	2099.7063.....	0.905	2122.7160.....	0.883
1096.6021.....	0.668	1102.5185.....	0.648	2099.7516.....	0.878		

Table 5 is also available in machine-readable form in the electronic edition of the *Astronomical Journal*.

TABLE 6

DIFFERENTIAL MAGNITUDES IN THE *I* BAND (VARIABLE MINUS COMPARISON)

HJD (2,450,000+)	ΔI (mag)	HJD (2,450,000+)	ΔI (mag)	HJD (2,450,000+)	ΔI (mag)	HJD (2,450,000+)	ΔI (mag)
1046.6381.....	0.715	1096.6013.....	0.751	1103.5937.....	1.542	2099.7741.....	0.958
1054.6805.....	0.741	1096.6812.....	0.737	1107.4955.....	1.391	2099.8043.....	0.923
1055.6323.....	0.834	1096.6984.....	0.741	1108.5285.....	0.722	2099.8520.....	0.876
1057.6029.....	0.796	1096.7129.....	0.745	1109.5068.....	0.862	2099.8787.....	0.852
1058.5754.....	0.751	1096.7425.....	0.732	1110.4876.....	0.725	2100.7509.....	0.737
1059.5779.....	0.791	1096.7557.....	0.739	1111.5065.....	0.855	2100.8158.....	0.739
1061.5672.....	0.770	1097.5856.....	0.903	1111.6442.....	0.768	2101.7485.....	1.188
1061.7719.....	0.764	1097.5977.....	0.922	1112.4893.....	0.713	2101.7529.....	1.130
1067.6474.....	0.718	1097.6027.....	0.930	1114.5107.....	0.773	2101.8490.....	0.870
1068.5822.....	0.829	1097.6163.....	0.936	1116.4754.....	0.761	2101.8534.....	0.865
1068.7284.....	1.255	1097.6441.....	0.965	1117.4872.....	0.782	2102.7101.....	0.708
1070.5545.....	0.841	1097.6580.....	0.968	1118.4737.....	0.783	2102.7146.....	0.744
1075.5296.....	0.708	1097.6709.....	0.975	1127.5324.....	0.708	2102.7485.....	0.729
1079.5560.....	0.717	1097.6809.....	0.980	1129.4726.....	0.718	2103.7067.....	0.891
1080.5458.....	1.284	1097.6913.....	0.998	1130.4667.....	1.544	2103.7111.....	0.866
1083.5944.....	0.747	1097.7016.....	1.008	1133.4938.....	0.732	2103.7473.....	0.861
1083.7240.....	0.789	1097.7147.....	1.011	1136.4862.....	0.870	2103.8185.....	0.794
1085.5387.....	0.681	1097.7243.....	1.011	1142.4637.....	0.768	2103.8229.....	0.800
1086.5435.....	0.797	1097.7352.....	1.016	1149.5121.....	0.827	2118.8890.....	1.007
1088.6404.....	0.782	1097.7463.....	1.019	1157.4476.....	1.561	2119.6908.....	0.726
1089.5240.....	0.764	1097.7614.....	1.037	1162.4514.....	0.701	2119.7196.....	0.737
1095.6525.....	1.082	1097.7713.....	1.026	1164.4451.....	0.746	2119.8360.....	0.709
1095.6750.....	1.145	1098.6142.....	0.739	1166.4341.....	0.715	2119.8701.....	0.712
1095.6886.....	1.195	1098.7044.....	0.725	1170.4433.....	0.756	2120.6915.....	1.095
1095.7002.....	1.240	1098.7183.....	0.745	1173.4446.....	0.745	2120.7275.....	1.239
1095.7078.....	1.274	1098.7327.....	0.734	1178.4536.....	0.813	2120.7814.....	1.456
1095.7142.....	1.303	1099.6184.....	1.492	1179.4499.....	0.739	2120.8153.....	1.567
1095.7239.....	1.338	1099.6327.....	1.560	1180.4521.....	1.079	2120.8551.....	1.639
1095.7309.....	1.374	1100.5892.....	0.729	2097.8012.....	1.522	2120.8741.....	1.610
1095.7544.....	1.466	1100.6072.....	0.727	2097.8384.....	1.405	2121.6997.....	0.725
1095.7644.....	1.500	1101.5894.....	1.019	2097.8637.....	1.308	2121.7603.....	0.723
1095.7757.....	1.537	1101.6130.....	1.019	2098.7261.....	0.703	2121.7969.....	0.713
1095.7841.....	1.564	1101.6195.....	1.002	2099.7072.....	1.000	2121.8543.....	0.708
1095.7900.....	1.586	1102.5163.....	0.712	2099.7524.....	0.978	2122.7168.....	0.982

Table 6 is also available in machine-readable form in the electronic edition of the *Astronomical Journal*.

TABLE 7
RADIAL VELOCITY MEASUREMENTS IN THE BARYCENTRIC FRAME

HJD (2,450,000+)	Phase	RV_1 (km s^{-1})	$(O-C)^a$ (km s^{-1})	RV_2 (km s^{-1})	$(O-C)^a$ (km s^{-1})	HJD (2,450,000+)	Phase	RV_1 (km s^{-1})	$(O-C)^a$ (km s^{-1})	RV_2 (km s^{-1})	$(O-C)^a$ (km s^{-1})
1013.6762.....	0.67797	−12.69	−0.35	−167.52	−0.33	1832.7380.....	0.23068	−117.98	+1.54	+51.27	+1.19
1057.7128.....	0.10580	−97.35	+0.94	+11.43	+3.06	1834.6800.....	0.73464	−7.16	−0.23	−191.51	−14.57
1087.6293.....	0.86936	−21.74	+0.16	−152.81	−4.88	1861.6437.....	0.73192	−8.18	−1.15	−170.73	+6.02
1089.6192.....	0.38575	−101.86	−1.34	+8.13	−7.09	1883.6075.....	0.43169	−85.09	+1.68	−2.57	+8.49
1092.6322.....	0.16765	−115.69	−3.15	+28.18	−8.70	1892.6091.....	0.76768	−2.49	+4.55	−177.64	−0.87
1118.6437.....	0.91783	−37.24	−1.85	−117.53	+3.00	2038.9430.....	0.74242	−4.21	+2.53	−179.70	−2.41
1119.6044.....	0.16714	−112.60	−0.14	+39.47	+2.76	2069.9033.....	0.77686	−2.75	+4.76	−178.99	−3.09
1120.6039.....	0.42652	−87.76	+0.72	−5.81	+2.33	2071.9200.....	0.30020	−116.00	+1.09	+47.77	+2.09
1121.6716.....	0.70359	−8.50	+0.54	−177.28	−4.16	2094.9643.....	0.28037	−116.87	+2.00	+40.30	−8.58
1122.6458.....	0.95641	−40.53	−2.58	−107.23	−12.61	2156.7515.....	0.31462	−116.73	−1.46	+42.92	+0.51
1177.5912.....	0.21515	−116.54	+2.04	+33.38	−14.98	2158.7204.....	0.82556	−11.88	+1.12	−168.54	−3.02
1325.9749.....	0.72184	−5.62	+1.93	−181.24	−5.43	2179.7118.....	0.27299	−119.13	+0.18	+58.71	+9.03
1352.9211.....	0.71458	−6.36	+1.69	−180.48	−5.58	2181.6579.....	0.77802	−6.69	+0.89	−177.49	−1.72
1356.9696.....	0.76520	−5.89	+1.06	−170.02	+6.91	2210.5986.....	0.28834	−117.01	+1.25	+28.68	−19.09
1360.8701.....	0.77740	−6.30	+1.23	−178.75	−2.89	2212.6412.....	0.81842	−10.83	+1.06	−170.16	−2.51
1446.6958.....	0.04982	−83.36	+5.48	−16.38	+10.95	2214.6180.....	0.33141	−113.45	−0.83	+36.14	−1.50
1447.6498.....	0.29739	−119.33	−1.92	+27.58	−18.68	2237.6534.....	0.30927	−115.84	+0.16	+53.52	+9.81
1472.6456.....	0.78399	−8.18	−0.20	−181.09	−6.07	2241.6129.....	0.33679	−112.38	−0.73	+39.30	+3.41
1474.6281.....	0.29846	−116.85	+0.45	+35.14	−10.91	2245.5893.....	0.36869	−106.32	−1.51	+13.87	−9.47
1476.6146.....	0.81397	−9.38	+1.84	−164.40	+4.52	2422.9568.....	0.39690	−94.62	+2.74	+10.14	+1.03
1505.6310.....	0.34395	−108.85	+1.45	+25.89	−7.56	2449.8731.....	0.38188	−101.79	−0.32	+27.62	+10.58
1507.6423.....	0.86590	−22.10	−1.01	−148.03	+1.53	2532.7302.....	0.88392	−27.44	−1.76	−145.43	−5.13
1509.5812.....	0.36905	−103.90	+0.86	+20.93	−2.32	2534.7906.....	0.41861	−86.86	+4.02	−5.63	−1.86
1534.5908.....	0.85923	−19.21	+0.34	−156.82	−4.17	2567.6127.....	0.93619	−40.95	−3.45	−107.78	+0.54
1653.9788.....	0.84132	−13.59	+2.21	−161.19	−1.12	2596.5941.....	0.45708	−80.72	−2.50	−25.54	−0.73
1682.9484.....	0.35915	−107.48	−0.41	+31.29	+3.75	2603.6793.....	0.29574	−120.22	−2.66	+39.56	−6.95
1684.9501.....	0.87860	−25.13	−0.89	−140.33	+2.88	2747.9926.....	0.74613	−4.32	+2.37	−180.16	−2.78
1686.9618.....	0.40065	−94.85	+1.47	+9.64	+2.56	2749.9920.....	0.26499	−117.51	+2.14	+38.92	−11.38
1709.8883.....	0.35025	−110.36	−1.35	+28.49	−2.60	2828.9094.....	0.74465	−6.58	+0.12	−176.21	+1.15
1711.8888.....	0.86940	−22.05	−0.11	−154.91	−7.06	2888.7413.....	0.27148	−122.02	−2.64	+31.85	−17.96
1740.8533.....	0.38590	−99.91	+0.53	+17.57	+2.50	2894.7945.....	0.84233	−17.75	−1.71	−163.79	−4.21
1742.8652.....	0.90801	−37.12	−4.68	−135.98	−9.43	2925.6356.....	0.84583	−17.72	−0.98	−166.13	−7.92
1803.8191.....	0.72600	−6.15	+1.15	−167.68	+8.57	2952.6175.....	0.84783	−18.90	−1.75	−170.13	−12.73
1805.8237.....	0.24621	−118.48	+1.43	+40.69	−10.09	2959.6194.....	0.66488	−17.93	−3.46	−160.13	+3.23

Table 7 is also available in machine-readable form in the electronic edition of the *Astronomical Journal*.
[a] Calculated from the simultaneous photometric and spectroscopic solution.

lines of the cooler component, whereas the earlier F8 type (from classification at shorter wavelengths) is more a reflection of the hotter primary. The light ratio between the primary and secondary was estimated from our spectra following Zucker & Mazeh (1994). We obtained $l_2/l_1 = 0.25 \pm 0.05$ at the mean wavelength of our spectroscopic observations (5187 Å), which is not far from the V band.

Instrumental shifts in velocity from run to run were monitored and corrected by taking frequent exposures of the dusk and dawn sky, in the manner described by Latham (1992). Systematic errors in our velocities due to the narrow spectral window were carefully checked and corrected for by means of numerical simulations following Torres et al. (2003). The corrections are typically under 1 km s^{-1} for the primary star and somewhat larger for the secondary. The final radial velocities for AV Del are listed in Table 7. A spectroscopic orbital solution (standard Keplerian fit) using these velocities gives the elements listed in Table 8, where the ephemeris adopted is that in equation (1). The increased scatter in the velocities of the secondary (some 4 times larger than the primary) is again due to the much weaker lines and higher rotational broadening of that component. The eccentricity of the orbit was found to be insignificant, as expected from the characteristics of the system. However, this fit does not account for the distortions in the stars

TABLE 8
SPECTROSCOPIC ORBITAL ELEMENTS OF AV DEL

Parameter	Value
P (days)[a]	3.8534528 ± 0.0000035 (fixed)
γ (km s^{-1})	−63.14 ± 0.24
K_1 (km s^{-1})	56.90 ± 0.30
K_2 (km s^{-1})	114.64 ± 1.15
e	0 (fixed)
Min. I (HJD)[a]	2,450,714.34779 ± 0.00039 (fixed)
$a_1 \sin i$ (10^6 km)	3.015 ± 0.016
$a_2 \sin i$ (10^6 km)	6.074 ± 0.062
$a \sin i$ ($R_\odot$)	13.059 ± 0.092
$M_1 \sin^3 i$ ($M_\odot$)	1.347 ± 0.032
$M_2 \sin^3 i$ ($M_\odot$)	0.668 ± 0.011
$q \equiv M_2/M_1$	0.4963 ± 0.0057
N_{obs}	68
Time span (days)	1945.9
σ_{RV_1} (km s^{-1})	2.05
σ_{RV_2} (km s^{-1})	7.96

[a] From ephemeris in eq. (1).

TABLE 9

PARAMETERS OF THE COMBINED RADIAL VELOCITY AND LIGHT-CURVE SOLUTIONS

Parameter	*B* Solution	*V* Solution	*R* Solution	*I* Solution	Semidetached *BVRI* Solution	Detached *BVRI* Solution
Geometric Parameters						
i (deg)	81.06 ± 0.20	81.07 ± 0.12	81.42 ± 0.10	81.55 ± 0.16	81.344 ± 0.066	81.561 ± 0.099
$q \equiv M_2/M_1$	0.4925 ± 0.0042	0.4878 ± 0.0052	0.4874 ± 0.0046	0.4865 ± 0.0057	0.4852 ± 0.0035	0.4933 ± 0.0025
a ($R_\odot$)	13.29 ± 0.07	13.34 ± 0.10	13.34 ± 0.09	13.34 ± 0.10	13.36 ± 0.09	13.25 ± 0.08
Ω_1	5.71 ± 0.15	5.68 ± 0.10	5.54 ± 0.11	5.78 ± 0.15	5.581 ± 0.048	5.838 ± 0.050
Ω_2[a]	2.861 ± 0.015	2.852 ± 0.015	2.852 ± 0.015	2.850 ± 0.015	2.847 ± 0.015	2.879 ± 0.005
$r_{\rm point}$ (pri, sec)	0.1935, 0.4277	0.1947, 0.4268	0.1999, 0.4267	0.1906, 0.4265	0.1983, 0.4262	0.1888, 0.3920
$r_{\rm pole}$ (pri, sec)	0.1913, 0.2986	0.1925, 0.2978	0.1974, 0.2978	0.1886, 0.2976	0.1959, 0.2974	0.1868, 0.2959
$r_{\rm side}$ (pri, sec)	0.1923, 0.3116	0.1935, 0.3108	0.1985, 0.3107	0.1895, 0.3106	0.1970, 0.3104	0.1877, 0.3085
$r_{\rm back}$ (pri, sec)	0.1932, 0.3441	0.1944, 0.3433	0.1996, 0.3433	0.1904, 0.3431	0.1980, 0.3429	0.1886, 0.3393
$r_{\rm 1vol}$[b]	0.1923 ± 0.0055	0.1935 ± 0.0038	0.1985 ± 0.0042	0.1895 ± 0.0055	0.1970 ± 0.0019	0.1877 ± 0.0018
$r_{\rm 2vol}$[b]	0.3181 ± 0.0042	0.3173 ± 0.0046	0.3171 ± 0.0044	0.3170 ± 0.0048	0.3169 ± 0.0040	0.3146 ± 0.0019
$\Delta\phi$	−0.00041 ± 0.00019	+0.00019 ± 0.00015	−0.00021 ± 0.00013	−0.00015 ± 0.00021	−0.00007 ± 0.00009	−0.00009 ± 0.00009
Radiative Parameters						
T_1 (K)	6000	6000	6000	6000	6000	6000
T_2 (K)	4195 ± 28	4270 ± 15	4264 ± 13	4289 ± 18	4275 ± 8	4277 ± 9
$L_{1,B}$[c]	0.7787 ± 0.0114	...	...	...	0.7635 ± 0.0042	0.7487 ± 0.0040
$L_{1,V}$[c]	...	0.6815 ± 0.0078	...	...	0.6883 ± 0.0042	0.6708 ± 0.0039
$L_{1,R}$[c]	...	...	0.6168 ± 0.0094	...	0.6107 ± 0.0047	0.5915 ± 0.0043
$L_{1,I}$[c]	...	...	...	0.5222 ± 0.0125	0.5450 ± 0.0049	0.5251 ± 0.0046
Albedo	0.5, 0.5	0.5, 0.5	0.5, 0.5	0.5, 0.5	0.5, 0.5	0.5, 0.5
Gravity brightening	0.36, 0.34	0.36, 0.34	0.36, 0.34	0.36, 0.34	0.36, 0.34	0.36, 0.34
Limb-Darkening Coefficients (Linear Law)						
x_B (pri, sec)	0.713, 1.008	...	...	...	0.713, 0.998	0.713, 0.997
x_V (pri, sec)	...	0.571, 0.840	...	...	0.571, 0.839	0.571, 0.839
x_R (pri, sec)	...	...	0.465, 0.689	...	0.465, 0.688	0.465, 0.687
x_I (pri, sec)	...	...	...	0.378, 0.551	0.378, 0.552	0.378, 0.552
$x_{\rm bolo}$ (pri, sec)	0.489, 0.528	0.489, 0.531	0.489, 0.531	0.489, 0.532	0.489, 0.532	0.489, 0.532
Other Quantities Pertaining to the Fit						
σ_B (mag)	0.023	...	...	...	0.029	0.026
σ_V (mag)	...	0.019	...	...	0.020	0.021
σ_R (mag)	...	...	0.014	...	0.015	0.015
σ_I (mag)	...	...	...	0.017	0.017	0.017
σ_{RV_1} (km s^{-1})	1.96	1.98	2.01	1.99	2.01	1.96
σ_{RV_2} (km s^{-1})	7.48	7.44	7.44	7.47	7.45	7.55
$N_{\rm obs}$ (phot.)	268	274	275	272	681	681
$N_{\rm obs}$ (spec.)	68	68	68	68	68	68

[a] The error for the semidetached case is derived from solutions in which the mass ratio q was varied over the range allowed by its error ($\pm 1\ \sigma$).
[b] Relative radius of a sphere with the same volume as the distorted star.
[c] Fractional luminosity of the primary.

and other effects, which are modeled more completely in the next section.

5. COMBINED PHOTOMETRIC AND SPECTROSCOPIC ANALYSIS

Examination of the raw light curves for AV Del does not reveal any obvious changes between the 1998–1999 and 2001–2002 observing seasons, so all data were combined with the spectroscopic observations and analyzed using the Wilson-Devinney code (Wilson & Devinney 1971; Wilson 1979, 1990). Solutions were found for the inclination angle (i), the semimajor axis (a), the center-of-mass velocity (γ), the mass ratio ($q \equiv M_2/M_1$), the modified gravitational potentials (Ω, in the Wilson-Devinney usage), the relative monochromatic luminosity of the primary (L_1), the mean temperature of the secondary (T_2), and a phase offset ($\Delta\phi$). The temperature of the primary was held fixed at the spectroscopic value of $T_1 = 6000$ K. The monochromatic luminosity of the secondary (L_2) was computed by the program directly from the temperatures of the primary and secondary, the luminosity of the primary, the radiation laws, and the geometry of the system. Limb-darkening coefficients were interpolated from the tables by van Hamme (1993) for the appropriate temperatures and for the surface gravities of $\log g_1 = 3.5$ and $\log g_2 = 3.0$. A value of 0.5 was adopted for the bolometric albedo of both components, appropriate for stars with convective envelopes. Gravity-brightening coefficients were interpolated from models by Claret (2000).

We initially obtained solutions in a mode appropriate for semidetached systems, following the expectation from the characteristics of AV Del. Specifically, we used "mode 5" for a secondary that is filling its limiting lobe. However, solutions were also tried for detached, contact, and overcontact configurations for completeness. Solutions using contact and overcontact configurations never resulted in satisfactory fits to the observations; however, a valid solution was obtained for a detached configuration with the secondary star slightly underfilling its limiting lobe (approximately 99% by radius).

Light-curve solutions were combined with the radial velocity data to give the added advantage of being able to model spectroscopic data that are affected by the Rossiter effect and other non-Keplerian distortions. Initial solutions were obtained separately for each bandpass to evaluate the consistency between them. The results were found to be reasonably similar, so solutions were then obtained for the combined *BVRI* data. The light elements from these fits are given in Table 9. We show the separate fits for each filter (semidetached case), as well as the simultaneous analysis of all four bands. The last column shows the simultaneous multiband analysis that resulted in a detached configuration. Also listed are the fractional radii ($r_{\rm point}$, $r_{\rm pole}$, $r_{\rm side}$, and $r_{\rm back}$, in terms of separation) and the relative radius of a spherical star with the same volume as the distorted stars ($r_{\rm vol}$) for the primary and secondary. The uncertainties given in these tables are standard errors as reported by the Wilson-Devinney code. Experiments were also carried out to investigate the significance of third light. No valid solutions were obtained when third light was added as an adjustable parameter. Similarly, fits allowing for a nonzero value of the eccentricity gave results consistent with a circular orbit, in agreement with the indications from spectroscopy.

Both eclipses for AV Del are partial, with approximately 45% of the light of the primary being blocked at phase 0.0. That star is well within its Roche lobe and is nearly spherical: the difference between the polar radius and the radius directed toward the inner Lagrangian point is only about 1%. The same difference in the semidetached configuration for the lobe-filling secondary star is about 30%. For the solution resulting in a slightly detached system, the secondary star is still highly distorted, with a point-to-polar difference of about 24%. The pole, back, and side radii for this solution are about 99% of those of the semidetached solution, while the point radius is about 92%.

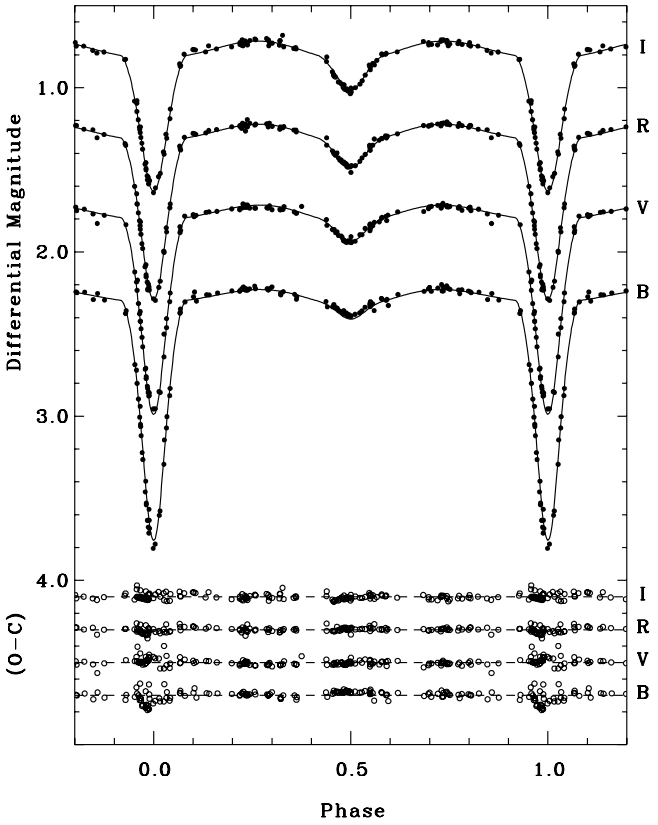

FIG. 2.—Light curves in *BVRI* for AV Del (displaced vertically for display purposes), along with our best fits for the semidetached case. Residuals are shown at the bottom.

A graphical representation of the observations is given in Figures 2 and 3 for the *BVRI* and radial velocity data, respectively, for the semidetached solution. (Analogous figures for the detached case are essentially indistinguishable.) The $O-C$ residuals are shown at the bottom of each figure. The errors in the fits are $\sigma = 0.029$, 0.020, 0.015, and 0.017 mag for the B, V, R, and I data, respectively, and 2.05 and 7.96 km s^{-1} for the primary and secondary radial velocities, respectively.

Finally, as mentioned earlier in § 2, an average time of primary eclipse was determined from the photometric observations by performing a separate fit with the Wilson-Devinney code in which all geometric and radiative elements were held fixed (semidetached case), with the exception of the time of eclipse (or phase correction $\Delta\phi$), which was allowed to vary. The *BVRI* passbands were used simultaneously. A similar exercise was carried out with the spectroscopy. The two estimates (constrained to be close to the average time of observation of each data set) are listed at the bottom of Table 1 and were used along with other timings from the literature to arrive at the final linear ephemeris in equation (1).

6. ABSOLUTE DIMENSIONS

The elements from the combined photometric and spectroscopic solution in Table 9 lead to the absolute masses, radii, and luminosities of the components of AV Del, along with other derived parameters. These quantities are listed in Table 10 for

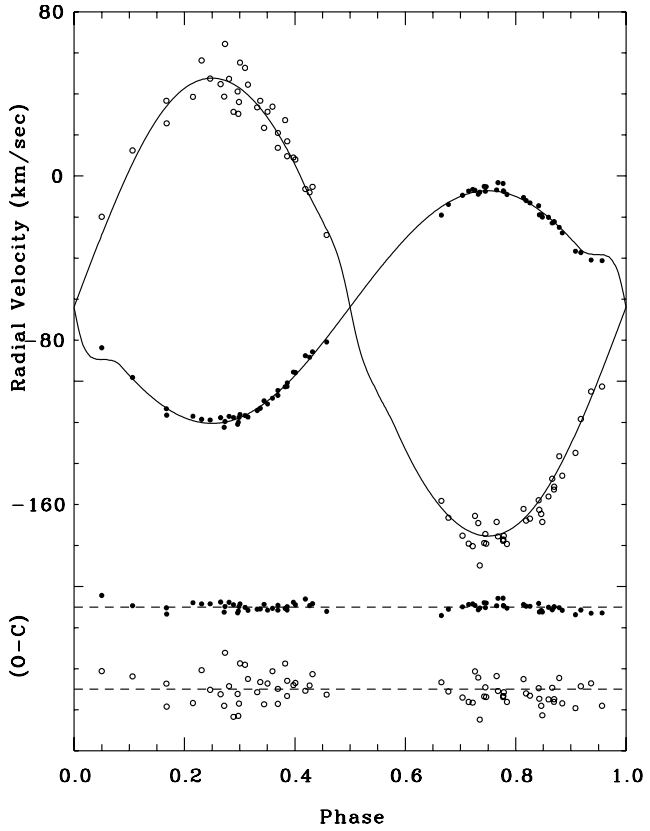

FIG. 3.—Radial velocity observations for AV Del shown with the best fit for the semidetached case. Filled circles represent the more massive primary star. Residuals are shown at the bottom.

TABLE 10

SUMMARY OF PHYSICAL PROPERTIES FOR AV DEL

Parameter	Primary	Secondary
Semidetached Solution		
M ($M_\odot$)	1.453 ± 0.028	0.705 ± 0.014
R ($R_\odot$)	2.632 ± 0.030	4.233 ± 0.060
$\log g$	3.759 ± 0.009	3.032 ± 0.010
$T_{\rm eff}$ (K)	6000 ± 200	4275 ± 150
$\bar{\rho}$ (g cm^{-3})[a]	0.1122 ± 0.0032	0.0131 ± 0.0005
$v_{\rm sync} \sin i$ (km s^{-1})[b]	34.2 ± 0.4	55.0 ± 0.8
$\log L_{\rm bol}$ ($L_\odot$)	0.906 ± 0.059	0.732 ± 0.062
$(L_2/L_1)_{\rm bol}$	0.67 ± 0.14	
$M_{\rm bol}$ (mag)	2.47 ± 0.15	2.90 ± 0.16
M_V (mag)	2.51 ± 0.18	3.69 ± 0.31
$m - M$ (mag)[c]	9.27 ± 0.19	
Distance (pc)[c]	710 ± 60	
Detached Solution		
M ($M_\odot$)	1.409 ± 0.027	0.695 ± 0.013
R ($R_\odot$)	2.487 ± 0.028	4.168 ± 0.036
$\log g$	3.795 ± 0.009	3.040 ± 0.005
$T_{\rm eff}$ (K)	6000 ± 200	4275 ± 150
$\bar{\rho}$ (g cm^{-3})[a]	0.1290 ± 0.0037	0.0135 ± 0.0002
$v_{\rm sync} \sin i$ (km s^{-1})[b]	32.3 ± 0.4	54.2 ± 0.5
$\log L_{\rm bol}$ ($L_\odot$)	0.857 ± 0.059	0.719 ± 0.061
$(L_2/L_1)_{\rm bol}$	0.73 ± 0.15	
$M_{\rm bol}$ (mag)	2.59 ± 0.15	2.94 ± 0.15
M_V (mag)	2.63 ± 0.18	3.72 ± 0.31
$m - M$ (mag)[c]	9.17 ± 0.19	
Distance (pc)[c]	680 ± 60	

[a] Mean stellar density.

[b] Projected rotational velocity assuming synchronous rotation.

[c] Assumes a total apparent magnitude of $V = 11.80 \pm 0.05$ and an extinction of $A_V = 0.34 \pm 0.10$ (see text).

both the semidetached and detached configurations. The absolute masses have relative errors formally under 2%, while the radii are good to better than 1.5%. The absolute visual magnitudes were derived here from the bolometric magnitudes using bolometric corrections (BCs) taken from Flower (1996) for the estimated temperatures of each component, with adopted uncertainties of 0.05 mag for BC. There appears to be no accurate measurement of the apparent visual magnitude of the system. Based on the estimate from the Tycho-2 Catalog (Høg et al. 2000), as well as measurements reported by Rapaport et al. (2001) and Skiff (2003), all transformed to the Johnson system, we adopted here $V = 11.80 \pm 0.05$ as a consensus value. The extinction toward AV Del is unknown but is likely to be nonnegligible. A rough estimate was obtained using the prescription by Hakkila et al. (1997) for the Galactic coordinates of the star ($l = 57^\circ$, $b = -19^\circ$) and an initial approximation of the distance, yielding $A_V = 0.34$ mag. We assign to this an arbitrary uncertainty of 0.1 mag. The resulting final distance estimate is approximately 700 pc.

The brightness ratios in the visual band $(L_2/L_1)_V$ that one may derive from the absolute visual magnitudes in Table 10, which are 0.34 ± 0.12 and 0.37 ± 0.13 for the semidetached and detached cases, respectively, are in fair agreement with the more precise values resulting from the light curve (0.45 ± 0.01 and 0.49 ± 0.01) and are also consistent with the spectroscopic value in § 4 of 0.25 ± 0.05 at a slightly bluer wavelength. However, the latter estimate seems smaller than the light-curve values.

If we assume that the rotation of each star is synchronized with the orbital motion, as expected for a system of this nature, the projected rotational velocities inferred from the measured radii (semidetached case) are 34.2 ± 0.4 and 55.0 ± 0.8 km s^{-1} for the primary and secondary, respectively. These are in excellent agreement with the measured values of 35 ± 1 and 56 ± 3 km s^{-1}. The agreement is not quite as good for the detached configuration (see Table 10).

7. DISCUSSION AND CONCLUDING REMARKS

Aside from better agreement with the measured projected rotational velocities mentioned above, there is little other information to decide which of the two configurations—detached or semidetached—the system is actually in. The quality of the fits to the photometry and radial velocities is similar. On physical grounds one might expect systems with these characteristics to be semidetached and in the process of transferring mass, but the detached configuration cannot be completely ruled out with the data in hand. The resulting masses and radii in the latter case are a few percent smaller than in the semidetached case. Thus, although likely, the status of AV Del as a bona fide member of the cool Algol class is not completely certain and should be confirmed with further observations or perhaps more direct evidence of mass transfer.

In binary systems of the Algol class the hotter star (mass gainer) appears to have adjusted to the mass transfer so that it displays physical properties typical of normal stars of the same mass. Similar characteristics are shown by the primary of AV Del. This is seen in Figure 4, where the luminosity derived from the effective temperature and measured radius (*filled circle with error box*) is compared with an evolutionary track (*solid line*) from the Yonsei-Yale series (Yi et al. 2001, 2003) for the exact

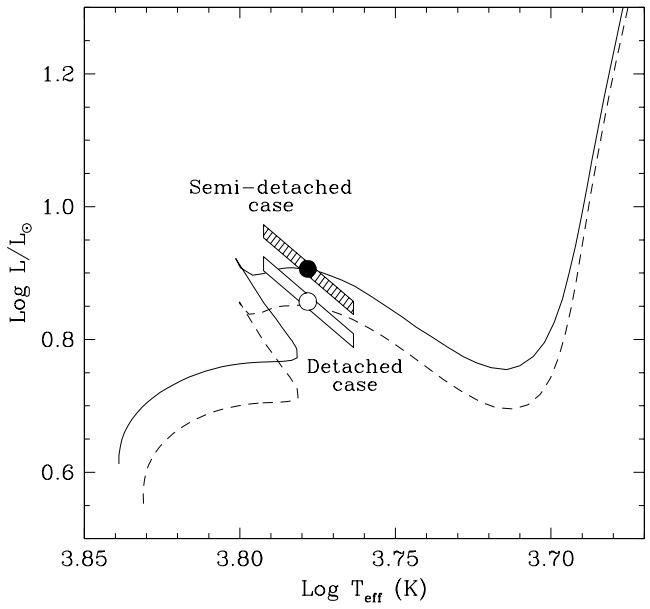

FIG. 4.—Primary component of AV Del in the H-R diagram, compared with an evolutionary track computed for the exact mass measured for the star (Yi et al. 2001, 2003) and for a metal abundance of $Z = 0.020$. We show the comparison for the semidetached case (*filled circle and solid line*) and the detached case (*open circle and dashed line*), both of which show good agreement with the models. Error boxes are based on the radius and temperature uncertainties in Table 10.

mass determined for the primary ($M_1 = 1.453\ M_\odot$; semidetached case) and a metal abundance very close to solar ($Z = 0.020$). The agreement is excellent and would appear to indicate that the star is in an evolutionary state similar to normal stars that are burning hydrogen in a shell. However, this interpretation is sensitive to some of the ingredients of the evolutionary models, in particular the convective core overshooting (see Demarque et al. 2004). An increase in this parameter would change the extent of the main sequence and might place the star at the end of the core hydrogen-burning stage instead. For comparison we show also the results

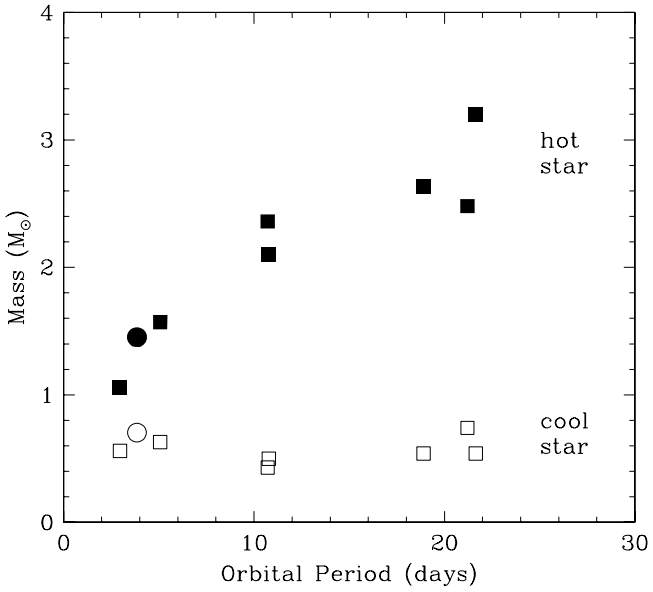

FIG. 5.—Mass-period relation for the components of all cool Algols for which estimates are available (see text). The results for AV Del from this paper are shown as circles. The cooler secondaries are all seen to have similar masses, while the primaries tend to be more massive in longer period systems.

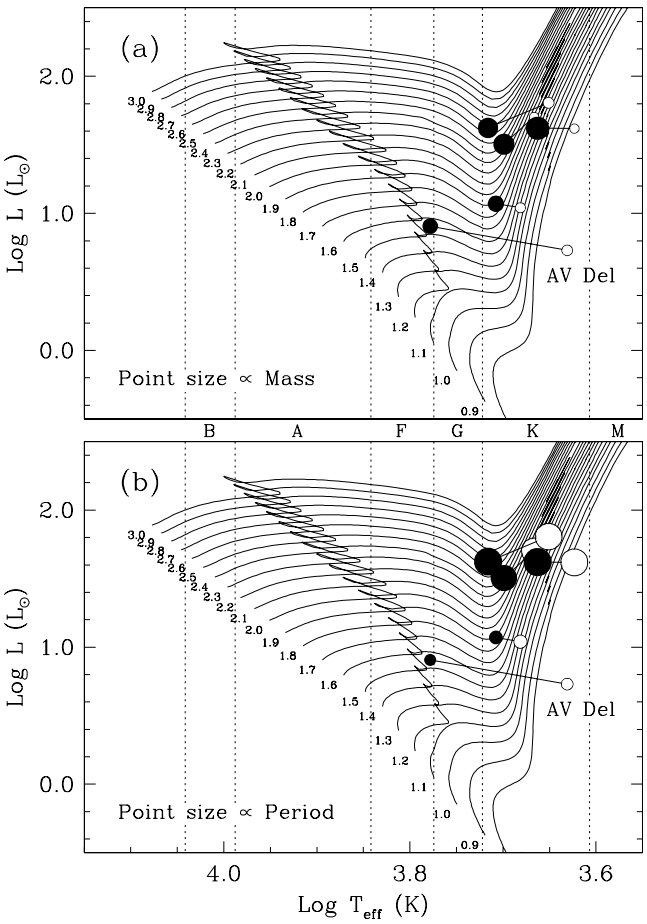

FIG. 6.—Primary and secondary components of the cool Algols having the most reliable parameters (RZ Cnc, AR Mon, RT Lac, and BD +05°706), along with AV Del, against the backdrop of evolutionary tracks by Yi et al. (2001, 2003) for metallicity $Z = 0.020$. Track masses in solar units are labeled on the left. Straight lines connect the hotter and more massive primaries (*filled circles*) with the secondaries (*open circles*) in each system. Spectral type boundaries are indicated with dashed lines. (*a*) Point size (area) proportional to the mass. (*b*) Point size (area) proportional to the orbital period.

for the detached configuration (*open circle and error box*), in which the primary mass and radius are about 3% and 6% smaller than the previous case, respectively. The track computed for the exact mass of the primary ($M_1 = 1.409\ M_\odot$ in this case) is shown with the dashed line and again provides a good fit.

As more detailed studies of cool Algols become available, some interesting general properties of this small class of binaries are emerging that may help piece together their evolutionary history. For example, we note that the mass of the cooler star in AV Del is quite similar to that of the mass-losing secondaries in all the other cool Algol systems for which estimates are available (RZ Cnc, AR Mon, RT Lac, AD Cap, RV Lib, BD +05°706, and V756 Sco; Popper 1976, 1991, 1996; Torres et al. 2003; Williamon et al. 2005). These components are all around $\sim$0.45 to $\sim$0.75 $M_\odot$ and are presumably in the process of being stripped to their helium cores. The hotter primary of AV Del, on the other hand, appears to follow the correlation with orbital period discussed by Torres et al. (1998), in the sense that systems with longer periods tend to have more massive primaries. These relations are displayed in Figure 5.

A further comparison with evolutionary tracks for single stars is shown in Figure 6, where we have included only the cool Algol systems with the most reliable estimates of the radius and temperature for both components (RZ Cnc, AR Mon, RT Lac,

and BD +05°706), along with AV Del. The tracks are from the same models used above, with the mass in solar units labeled on the left. Approximate spectral type boundaries are indicated with dotted lines. The primary and secondary stars (*filled and open circles, respectively*) in each binary are shown connected with a line. In the top panel the symbol size (area) is proportional to the mass of the star. The three more massive primaries are the more luminous, and all except for AV Del lie more or less at the base of the giant branch. AV Del has the hottest primary of the group, and as indicated above, that star appears to be at or just past the end of the hydrogen-burning phase for normal stars of similar mass. The mass-losing secondaries of all the cool Algols lie considerably to the right, not surprisingly at positions inconsistent with the evolution of single stars. The bottom panel of Figure 6 has the size (area) of the points proportional to the orbital period, showing the primaries in the wider orbits to be more luminous. It is tempting to infer from these diagrams a kind of evolutionary sequence for cool Algols, with AV Del being the least evolved of the five systems in that its primary has not yet reached the base of the giant branch corresponding to its mass. It is also the binary with the shortest period and smallest primary mass, and this may be significant given that the direction of mass transfer in these systems, from the less massive to the more massive star, would tend to make the period increase.

Our detailed photometric and spectroscopic analysis of AV Del has yielded the first precise determinations of the absolute properties of the system (masses, radii, luminosities, etc.), and this star is potentially an addition to the small but growing number of cool Algols subjected to similar studies. Although a semidetached configuration appears more likely for this binary, further observations are required to completely rule out an alternative detached status with the cooler secondary slightly underfilling its Roche lobe.

We thank the referee for helpful comments on the manuscript. We also thank Perry Berlind, Mike Calkins, Joe Caruso, Dave Latham, and Robert Stefanik for carrying out the spectroscopic observations of AV Del at CfA. Observations at NURO were conducted with the assistance of Stephanie Ferrari, Jeff McIntyre, Aaron Burgman, and Michael Seeds (Franklin and Marshall College), and Teddy George (Canada-France-Hawaii Telescope) assisted with the observations at McDonald Observatory. Support for this research was provided to L. M. by Gettysburg College and the Delaware Space Grant Consortium. G. T. acknowledges partial support from NSF grant AST 04-06183. This research has made use of the SIMBAD database, operated at CDS, Strasbourg, France, and of NASA's Astrophysics Data System Abstract Service.

REFERENCES

Agerer, F., & Hübscher, J. 1999, Inf. Bull. Variable Stars, 4711, 1
Claret, A. 2000, A&A, 359, 289
Demarque, P., Woo, J.-H., Kim, Y.-C., & Yi, S. K. 2004, ApJS, 155, 667
Diethelm, R. 1973, BBSAG Bull., 11
———. 1976a, BBSAG Bull., 27
———. 1976b, BBSAG Bull., 28
———. 1977, BBSAG Bull., 35
———. 1978, BBSAG Bull., 37
———. 1985, BBSAG Bull., 78
———. 1986, BBSAG Bull., 79
———. 1988, BBSAG Bull., 86
———. 1991, BBSAG Bull., 98
———. 1994, BBSAG Bull., 105
Flower, P. J. 1996, ApJ, 469, 355
Hakkila, J., Myers, J. M., & Stidham, B. J. 1997, AJ, 114, 2043
Halbedel, E. M. 1984, Inf. Bull. Variable Stars, 2549, 1
Hall, D. S. 1989, in IAU Coll. 107, Algols, ed. A. H. Battan (Dordrecht: Kluwer), 219
Hoffmeister, C. 1935, Astron. Nachr., 255, 401
Hoffmeister, C., Jensch, A., Morgenroth, O., van Schewick, H., Hoppe, J., & Miczaika, G. R. 1938, Klein Veröff. Univ. Berlin Babelsberg, 19, 1
Høg, E., et al. 2000, A&A, 355, L27
Kordylewski, K. 1963, Inf. Bull. Variable Stars, 35, 1
Kundera, T. 2004, Eclipsing Binaries Minima Database (Krakow: Obs. Astron. Uniw. Jagiellońksiego)
Latham, D. W. 1992, in IAU Coll. 135, Complementary Approaches to Double and Multiple Star Research, ed. H. A. McAlister & W. I. Hartkopf (ASP Conf. Ser. 32; San Francisco: ASP), 110
Popper, D. M. 1976, ApJ, 208, 142
———. 1980, in IAU Symp. 88, Close Binary Stars: Observations and Interpretations, ed. M. J. Plavec, D. M. Popper, & R. K. Ulrich (Dordrecht: Reidel), 387
———. 1991, AJ, 101, 220
———. 1992, in IAU Symp. 151, Evolutionary Processes in Interacting Binary Stars, ed. Y. Kondo, R. F. Sisteró, & R. S. Polidan (Dordrecht: Kluwer), 395
———. 1996, ApJS, 106, 133
Qian, S. 2002, Ap&SS, 282, 399
Rapaport, M., et al. 2001, A&A, 376, 325
Skiff, A. B. 2003, Catalogue of Stellar Spectral Classifications (Flagstaff: Lowell Obs.)
Torres, G., Mader, J. A., Marschall, L. A., Neuhäuser, R., & Duffy, A. S. 2003, AJ, 125, 3237
Torres, G., Neuhäuser, R., & Wichmann, R. 1998, AJ, 115, 2028
van Hamme, W. 1993, AJ, 106, 2096
Williamon, R. M., Van Hamme, W., Torres, G., Sowell, J. R., & Ponce, V. C. 2005, AJ, 129, 2798
Wilson, R. E. 1979, ApJ, 234, 1054
———. 1990, ApJ, 356, 613
Wilson, R. E., & Devinney, E. J. 1971, ApJ, 166, 605
Yi, S., Demarque, P., Kim, Y.-C., Lee, Y.-W., Ree, C. H., Lejeune, T., & Barnes, S. 2001, ApJS, 136, 417
Yi, S. K., Kim, Y.-C., & Demarque, P. 2003, ApJS, 144, 259
Zejda, M. 2004, Inf. Bull. Variable Stars, 5583, 1
Zucker, S., & Mazeh, T. 1994, ApJ, 420, 806